

Identifying Disruptive Contingencies for Catastrophic Cascading Failures in Power Systems

Chao Zhai, Gaoxi Xiao, Hehong Zhang, Peng Wang and Tso-Chien Pan *

April 2, 2020

Abstract

Due to the evolving nature and the complicated coupling relationship of power system components, it has been a great challenge to identify the disruptive contingencies that can trigger cascading blackouts. This paper aims to develop a generic approach for identifying the initial disruptive contingencies that can result in the catastrophic cascading failures of power systems. The problem of contingency identification is formulated in the mathematical framework of hybrid differential-algebraic system, and it can be solved by the Jacobian-Free Newton-Krylov method, which allows to circumvent the Jacobian matrix and relieve the computational burden. Moreover, an efficient numerical algorithm is developed to search for the disruptive contingencies that lead to catastrophic cascading failures with the guaranteed convergence accuracy in theory. Finally, case studies are presented to demonstrate the efficacy of the proposed identification approach on the IEEE test systems by using different cascade models.

Keywords: Cascading failures, contingency identification, Jacobian-Free Newton-Krylov method, power systems

*Chao Zhai is with the School of Automation, China University of Geosciences, Wuhan 430074 China, and with Hubei Key Laboratory of Advanced Control and Intelligent Automation for Complex Systems, Wuhan 430074, China. Gaoxi Xiao, Hehong Zhang, Peng Wang and Tso-Chien Pan are with Institute of Catastrophe Risk Management, Nanyang Technological University, 50 Nanyang Avenue, Singapore 639798. They are also with Future Resilient Systems, Singapore-ETH Centre, 1 Create Way, CREATE Tower, Singapore 138602. Gaoxi Xiao, Hehong Zhang and Peng Wang are with School of Electrical and Electronic Engineering, Nanyang Technological University, Singapore. Corresponding author: Gaoxi Xiao. Email: egxxiao@ntu.edu.sg

1 Introduction

The recent years have witnessed several large blackouts in the world such as Pakistan Blackout in January 2015 [1], Turkey Blackout in March 2015 [2], Canada Blackout in September 2016 [3], Brazil Blackout in March 2018 [4], and London Blackout in August 2019 [5], to name just a few. These blackouts have left millions of residents without power supply and caused huge financial losses [6]. In such catastrophe events, the initial disruptive contingencies (e.g. tree contact [7], flashover [8], equipment faults [9], etc) play a crucial role in triggering the cascading outage of power systems. Thus, it is vital to identify the initial disruptive contingencies that cause the catastrophic cascading failure so that remedial actions can be taken in advance to prevent the blackout [10].

To identify disruptive contingencies for catastrophic cascading failures, it is crucial to make practical cascading failure models of power systems and develop the effective identification approaches. So far, both the DC power flow model and the AC power flow model with transient process have been developed to describe the power system cascades [11, 12]. In addition, multiple identification approaches are proposed to search for critical branches or initial malicious disturbances that can cause the large-scale disruptions of power grids [13, 14, 15, 16, 17, 18, 19]. For instance, some approaches are proposed to identify the collections of $n - k$ contingencies via the event trees [13], line outage distribution factor [14] and other optimization techniques [15, 16, 17]. These approaches are not efficient to identify the large collections of $n - k$ contingencies that result in cascading blackouts. To deal with this issue, a “random chemistry” algorithm is designed with a relatively low computational complexity [18]. It is worth pointing out that these approaches focus on the direct branch outage as the disruptive contingencies without taking into account the continuous change of branch admittance caused by disruptive contingencies. In practice, many factors (e.g. temperature, short circuit, poor contactor, etc) may lead to the continuous changes of branch admittance [20]. By treating the contingencies as the control inputs, an optimal control approach is adopted to identify the disruptive contingencies, and it allows to determine the continuous changes of branch admittance in addition to direct branch outages [19]. Nevertheless, the above optimal control approach is only applied to the DC power flow models, and it can not deal with the AC power flow models with transient process. For this reason, it is necessary to develop a generic approach that can be applied to both the DC power flow models and the AC power flow models with transient process to characterize real physical characteristics of power system cascades. Moreover, the proposed approach is required to identify disruptive contingencies that give rise to the continuous changes of branch admittance in addition to the direct branch outages.

Therefore, this work takes a first step towards a generic approach for identifying disruptive contin-

gencies that cause the catastrophic cascading failures in power systems. Compared to existing work, the main contributions of this work are highlighted as follows

1. Propose a mathematical formulation of power system cascades that can allow for complicated intrinsic dynamics and various contingencies.
2. Develop a numerical algorithm based on the Jacobian-Free Newton-Krylov method for identifying catastrophic cascading failures in large-scale power systems with the guaranteed performance in theory.
3. Provide the insight into the real-time protection of power grids with the aid of various power system devices.

The remainder of this paper is organized as follows. Section 2 presents a general mathematical model of cascading failures and optimization formulation, followed by the numeric solver and theoretical analysis in Section 3. Next, case studies on the validation of the proposed approach are given in Section 4. Finally, we conclude the paper and discuss future work in Section 5.

2 Formulation of Contingency Identification for Power System Cascades

During the cascades, the initial disruptive contingency can result in the change of branch impedance or the direct branch outages. This may wake hidden failures of power grids or cause situational awareness errors of operators, and thus aggravate the stresses of power networks. If the stresses are not relieved, it will give rise to more branch outages and trigger protective actions (e.g., load shedding and generator tripping). In the worst case, the above chain reactions end up with the catastrophic cascading failures (see Figure 1). This section aims to formulate the problem of identifying the above catastrophic cascading failures of power grids. First of all, a general mathematical model is introduced to characterize the practical cascading failure of power grids subject to various disruptive contingencies. Then an optimization formulation is proposed to search for the disruptive contingencies, followed by the necessary conditions of the proposed optimization problem.

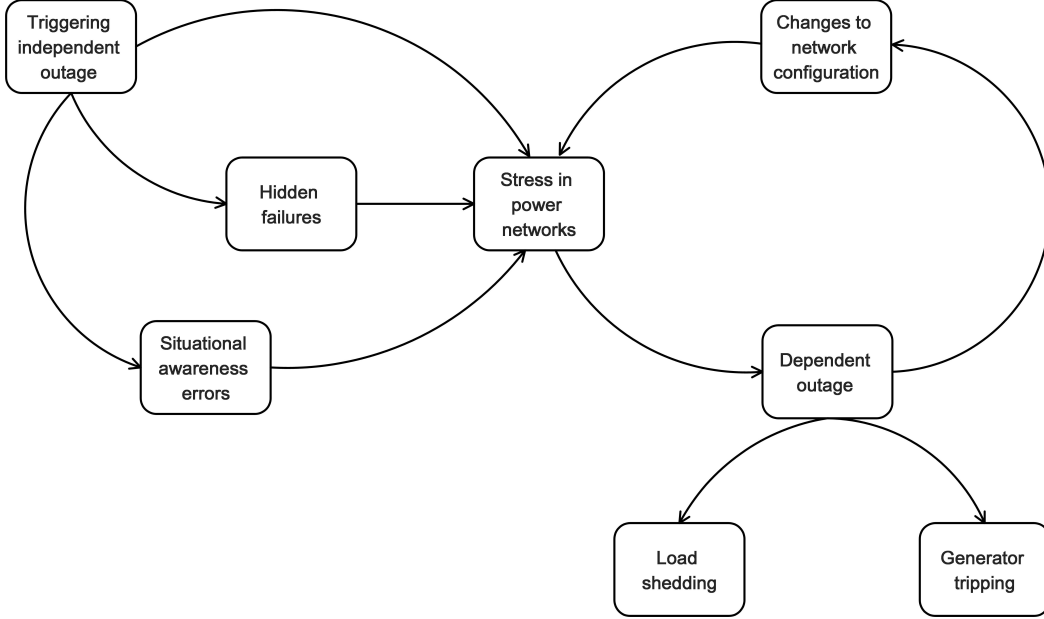


Figure 1: Cascading failure process of power grids [21].

2.1 Mathematical model of power system cascades

The cascading failure process of power systems can be modeled as a system of hybrid differential-algebraic equations [11].

$$\begin{cases} \dot{x} = f(t, x, y, \theta) \\ 0 = g(t, x, y, \theta) \\ 0 > h(t, x, y, \theta) \end{cases} \quad (1)$$

where x denotes a vector of continuous state variables subject to differential relationships, and y represents a vector of continuous state variables under the constraints of algebraic equations. In addition, θ refers to a vector of discrete binary state variables (i.e., $\theta_i \in \{0, 1\}$). The system of hybrid differential algebraic equations contribute to a general mathematical framework to describe the complicated process of cascading failures as well as various contingencies. The differential equations in the system (1) characterize the dynamic response of machines, governors, exciters and loads in power grids. The algebraic components mainly describe the AC power flow equations, and the inequality terms reflect the discrete events (e.g., the automatic line tripping by protective relays, manual operations, lightning, etc) during cascading failures. The discrete events refer to the branch outages in power systems. In practice, the structure of power grids (e.g., network topology, component parameters) is affected once a discrete event occurs. Thus, the discrete events directly influence the dynamic response of relevant devices and power flow distribution. To incorporate the effect of discrete events at time instants t_k , the time axis is

divided into a series of time intervals $[t_{k-1}, t_k)$, $k \in I_m = \{1, 2, \dots, m\}$. At each time interval, the set of differential-algebraic equations is solved using the updated parameters and initial conditions of power system model due to discrete events. By solving the system (1) in each time interval, the vectors of state variables x and y at the terminal of each time interval can be obtained by

$$\begin{cases} x_k = F(t_k, x_{k-1}, y_{k-1}, \theta_{k-1}) \\ y_k = G(t_k, x_{k-1}, y_{k-1}, \theta_{k-1}) \end{cases} \quad (2)$$

where $x_k = x(t_k)$, $y_k = y(t_k)$ and $\theta_k = \theta(t_k)$, $k \in I_m$. And the iterated functions F and G characterize the discrete-time evolution of state variables x_k and y_k , respectively. Equation (2) enables us to implement the numerical algorithm for identifying the disruptive contingencies.

2.2 Optimization formulation for identifying disruptive contingencies

The cascading blackouts may result in the large disruptions of power systems and paralyze the service of power supply. The objective of this work is to search for the initial disruptive contingencies that cause the catastrophic cascading failures. In theory, the problem of identifying initial disruptive contingencies can be formulated as

$$\begin{aligned} & \min_{\delta \in \Omega} J(\delta, x_m, y_m) \\ & s. t. \quad x_k = F(t_k, x_{k-1}, y_{k-1}, \theta_{k-1}) \\ & \quad y_k = G(t_k, x_{k-1}, y_{k-1}, \theta_{k-1}), \quad k \in I_m \end{aligned} \quad (3)$$

where δ denotes the disruptive contingencies that cause the changes of state variables x , y or θ in the initial time interval $[t_0, t_1)$. It can describe both single disturbance and multiple disturbances as the initial contingency. And Ω represents the set of n physical restrictions on initial contingencies, which can be described as $\bigcap_{i=1}^n \{\delta \mid v_i(\delta) \leq 0\}$ with the inequality constraints $v_i(\delta) \leq 0$. For simplicity, it is assumed that the triggering event or initial contingency occurs at time $\tau \in [t_0, t_1)$. Then we have $(x(\tau_+), y(\tau_+), \theta(\tau_+)) = \Gamma(x(\tau), y(\tau), \theta(\tau), \delta)$, and the function Γ characterizes the effect of the contingency δ on the state variables at time τ .

The objective function $J(\delta, x_m, y_m)$ quantifies the disruptive level of power grids at the end of cascading failures. A smaller value of $J(\delta, x_m, y_m)$ indicates a worse disruption of power grids due to cascading blackouts. In practice, the objective function is designed according to the definition of catastrophic cascading failure. For example, if the connectivity of power networks is concerned, it can be designed as $J(\delta, x_m, y_m) = \|Y_p^m\|^2$, where Y_p^m denotes the vector of branch admittance at the end of cascades. A smaller value of $\|Y_p^m\|^2$ indicates a worse connectivity of power networks. If the disruption level of cascades is

characterized by the power flow, it can be designed as $J(\delta, x_m, y_m) = \|P_e^m\|^2$, where P_e^m denotes the vector of power flow on branches at the end of cascades and it is related to Y_p^m and P^m . A smaller value of $\|P_e^m\|^2$ implies a weaker transmission capability of power flow. It follows from the Karush-Kuhn-Tucker (KKT) conditions that the necessary conditions for optimal solutions to Optimization Problem (3) is presented as follows [22].

Proposition 2.1. *The optimal solution δ^* to the Optimization Problem (3) with the multipliers μ_i , $i \in I_n$ satisfies the KKT conditions*

$$\begin{aligned} \nabla J(\delta^*, x_m, y_m) + \sum_{i=1}^n \mu_i \nabla v_i(\delta^*) &= \mathbf{0} \\ v_i(\delta^*) + \omega_i^2 &= 0 \\ \mu_i \cdot v_i(\delta^*) &= 0 \\ \mu_i - \sigma_i^2 &= 0, \quad i \in I_n \end{aligned} \quad (4)$$

where ω_i and σ_i , $i \in I_n$ are the unknown variables.

Proof. The KKT conditions for Optimization Problem (3) are composed of four components: stationary, primal feasibility, dual feasibility and complementary slackness. Specifically, stationary condition allows us to obtain

$$\nabla J(\delta^*, x_m, y_m) + \sum_{i=1}^n \mu_i \nabla v_i(\delta^*) = 0, \quad (5)$$

where

$$\Omega = \bigcap_{i=1}^n \{\delta \mid v_i(\delta) \leq 0\}. \quad (6)$$

Moreover, the primal feasibility leads to $g_i(\delta) \leq 0$, $i \in I_n$, which can be converted into equality constraints

$$v_i(\delta^*) + \omega_i^2 = 0, \quad i \in I_n \quad (7)$$

with the unknown variables $\omega_i \in \mathcal{R}$. Further, the dual feasibility corresponds to $\mu_i \geq 0$, which can be replaced by

$$\mu_i - \sigma_i^2 = 0, \quad i \in I_n \quad (8)$$

with the unknown variables $\sigma_i \in \mathcal{R}$. Finally, the complementary slackness gives

$$\mu_i \cdot v_i(\delta^*) = 0, \quad i \in I_n \quad (9)$$

This completes the proof. □

Remark 2.1. To reduce the computational burden, the gradient $\nabla J(\delta^*, x_m, y_m)$ can be approximated by

$$\begin{aligned} \nabla J(\delta, x_m, y_m)|_{\delta=\delta^*} &= \frac{\partial J(\delta, x_m, y_m)}{\partial \delta_i} \Big|_{\delta=\delta^*} \in \mathbf{R}^{\dim(\delta)} \\ &\approx \frac{J(\delta^* + \xi e_i, x_m, y_m) - J(\delta^*, x_m, y_m)}{\xi} \end{aligned} \quad (10)$$

with a sufficiently small ξ and the unit vector e_i with 1 in the i -th position and 0 elsewhere. And the symbol $\dim(\delta)$ denotes the dimension of the variable δ . By selecting a different unit vector e_i , Equation (10) can provide the gradient of objective function with respect to a different disturbance.

The continuous variable δ in the optimization problem (3) denotes the change of state variables of power systems caused by the initial disruptive contingencies. Essentially, θ is not an independent binary variable, and it is actually dependent on the continuous state variables x and y . In other words, θ is the function of x and y , and the optimization problem (3) is actually related to the continuous state variables. Thus, the KKT conditions are applicable to the optimization problem (3), and the non-continuity caused by θ can be handled by the Jacobian-Free Newton-Krylov (JFNK) method, as presented in the next section.

3 Numeric Solver for Identifying Disruptive Contingencies

This section presents the numerical algorithm based on JFNK method to identify the disruptive contingencies for catastrophic cascading failures. The JFNK method is introduced in the first place with the estimation of numerical error, followed by the corresponding numerical algorithm and theoretical results.

During the cascades, the branch outages result in the noncontinuous change of state variables in power systems, which makes it infeasible to directly compute partial derivatives for identifying the initial disruptive contingencies by the Jacobian matrix based methods [23]. For this reason, the Jacobian-Free Newton-Krylov method is employed to solve the system of nonlinear algebraic equations (4) without computing the Jacobian matrix. It also enables us to identify the catastrophic cascading failures caused by the continuous changes of branch admittance in addition to the direct branch outages. To facilitate the analysis, the system (4) can be rewritten in matrix form as follows

$$S(\mathbf{z}) = \mathbf{0}, \quad (11)$$

where the unknown vector \mathbf{z} is composed of δ^* , μ_i , ω_i , σ_i , $i \in I_n$. And $\mathbf{0}$ refers to a zero vector with the proper dimension. To obtain the iterative formula for solving (11), the Taylor series of $S(\mathbf{z})$ at \mathbf{z}^{s+1} is computed by

$$S(\mathbf{z}^{s+1}) = S(\mathbf{z}^s) + \tilde{\mathcal{J}}(\mathbf{z}^s)(\mathbf{z}^{s+1} - \mathbf{z}^s) + O(\Delta \mathbf{z}^s) \quad (12)$$

with $\Delta \mathbf{z}^s = \mathbf{z}^{s+1} - \mathbf{z}^s$. By neglecting the high-order term $O(\Delta \mathbf{z}^s)$ and setting $S(\mathbf{z}^{s+1}) = \mathbf{0}$, we obtain

$$\tilde{\mathfrak{J}}(\mathbf{z}^s) \cdot \Delta \mathbf{z}^s = -S(\mathbf{z}^s), \quad s \in Z^+ \quad (13)$$

where $\tilde{\mathfrak{J}}(\mathbf{z}^s)$ represents the Jacobian matrix and s denotes the iteration index. Equation (13) is used to obtain the iteration increment for numerical algorithm to solve the equation (11). Note that the Jacobian matrix $\tilde{\mathfrak{J}}$ is different from the objective function J in the optimization problem (3). Thus, solutions to Equation (11) can be approximated by implementing Newton iterations $\mathbf{z}^{s+1} = \mathbf{z}^s + \Delta \mathbf{z}^s$, where $\Delta \mathbf{z}^s$ is obtained by Krylov methods. The details of Krylov methods to compute $\Delta \mathbf{z}^s$ are elaborated as follows. First of all, the Krylov subspace is constructed by

$$K_i = \text{span}(\mathbf{r}^s, \tilde{\mathfrak{J}}(\mathbf{z}^s)\mathbf{r}^s, \tilde{\mathfrak{J}}(\mathbf{z}^s)^2\mathbf{r}^s, \dots, \tilde{\mathfrak{J}}(\mathbf{z}^s)^{i-1}\mathbf{r}^s) \quad (14)$$

with $\mathbf{r}^s = -S(\mathbf{z}^s) - \tilde{\mathfrak{J}}(\mathbf{z}^s) \cdot \Delta \mathbf{z}_0^s$, where $\Delta \mathbf{z}_0^s$ is the initial guess for the Newton correction and is typically zero [24]. Actually, the optimal solution to $\Delta \mathbf{z}^s$ is the linear combination of elements in Krylov subspace K_i

$$\Delta \mathbf{z}^s = \Delta \mathbf{z}_0^s + \sum_{j=1}^{i-1} \lambda_j \cdot \tilde{\mathfrak{J}}(\mathbf{z}^s)^j \mathbf{r}^s, \quad (15)$$

where $\lambda_j, j \in \{1, 2, \dots, i-1\}$ is obtained by minimizing the residual \mathbf{r}^s with the Generalized Minimal RESidual (GMRES) method, and $\Delta \mathbf{z}^s$ is subject to the constraint $\|\Delta \mathbf{z}^s\| \leq c$ [25]. In other words, Equation (15) allows to compute the iteration increment for solving Equation (11) with the minimum residual. In addition, the matrix-vector products in (15) can be approximated by

$$\tilde{\mathfrak{J}}(\mathbf{z}^s)\mathbf{r}^s \approx \frac{S(\mathbf{z}^s + \varepsilon \mathbf{r}^s) - S(\mathbf{z}^s)}{\varepsilon}, \quad (16)$$

where ε is a sufficiently small value [26]. In this way, the computation of Jacobian matrix is avoided via matrix-vector products in (16) while solving Equation (11). The accuracy of the forward difference scheme (16) can be estimated by the following proposition.

Proposition 3.1.

$$\left\| \frac{S(\mathbf{z}^s + \varepsilon \mathbf{r}^s) - S(\mathbf{z}^s)}{\varepsilon} - \tilde{\mathfrak{J}}(\mathbf{z}^s)\mathbf{r}^s \right\| \leq \frac{\varepsilon \|\mathbf{r}^s\|^2}{2} \sup_{t \in [0,1]} \|S^{(2)}(\mathbf{z}^s + t\varepsilon \mathbf{r}^s)\| \quad (17)$$

where $S^{(2)}(z)$ denotes the second order derivative of $S(z)$ with respect to the unknown vector z .

Proof. It follows from NR 3.3-3 in [27] that

$$\frac{S(\mathbf{z}^s + \varepsilon \mathbf{r}^s) - S(\mathbf{z}^s)}{\varepsilon} - \tilde{\mathfrak{J}}(\mathbf{z}^s)\mathbf{r}^s = \int_0^1 \varepsilon(1-t)S^{(2)}(\mathbf{z}^s + t\varepsilon \mathbf{r}^s)\mathbf{r}^s \mathbf{r}^s dt \quad (18)$$

which implies

$$\begin{aligned}
\left\| \frac{S(\mathbf{z}^s + \varepsilon \mathbf{r}^s) - S(\mathbf{z}^s)}{\varepsilon} - \tilde{\mathcal{J}}(\mathbf{z}^s) \mathbf{r}^s \right\| &= \left\| \int_0^1 \varepsilon (1-t) S^{(2)}(\mathbf{z}^s + t\varepsilon \mathbf{r}^s) \mathbf{r}^s \mathbf{r}^s dt \right\| \\
&\leq \varepsilon \int_0^1 (1-t) \left\| S^{(2)}(\mathbf{z}^s + t\varepsilon \mathbf{r}^s) \mathbf{r}^s \mathbf{r}^s \right\| dt \\
&\leq \varepsilon \int_0^1 (1-t) \|S^{(2)}(\mathbf{z}^s + t\varepsilon \mathbf{r}^s)\| \cdot \|\mathbf{r}^s\|^2 dt \\
&\leq \varepsilon \sup_{t \in [0,1]} \|S^{(2)}(\mathbf{z}^s + t\varepsilon \cdot \mathbf{r}^s)\| \cdot \|\mathbf{r}^s\|^2 \int_0^1 (1-t) dt \\
&= \frac{\varepsilon \|\mathbf{r}^s\|^2}{2} \sup_{t \in [0,1]} \|S^{(2)}(\mathbf{z}^s + t\varepsilon \mathbf{r}^s)\|
\end{aligned} \tag{19}$$

The proof is thus completed. \square

Remark 3.1. *The choice of ε greatly affects the accuracy and robustness of the JFNK method. For the forward difference scheme (16), ε can be set equal to a value larger than the square root of machine epsilon to minimize the approximation error [28].*

The JFNK method enables us to develop an efficient numerical algorithm for identifying disruptive contingencies, and Table 1 elaborates on the Contingency Identification Algorithm (CIA) based on the JFNK method. Before running the CIA, the initial values for some variables are specified as follow: $\delta = l = 0$, ε_{\min} , ε_0 with the condition $\varepsilon_{\min} < \varepsilon_0$, and the maximum iterative step l_{\max} . Then the JFNK method is employed to obtain the optimal disturbance δ^* and the cost $J(\delta^*, x_m, y_m)$ from Step 4 to Step 16. Specifically, the residual \mathbf{r}^s is calculated in each iteration in order to construct the Krylov subspace K_i . For elements in K_i , the matrix-vector products are approximated by Equation (16) without forming the Jacobian. Next, the term $\Delta \mathbf{z}^s$ for Newton iterations is obtained via the GMRES method [25]. The tolerance ε_s and step number s are updated after implementing the Newton iteration for \mathbf{z}^s . Afterwards, a new iteration loop is launched if the termination condition $\varepsilon_s \leq \varepsilon_{\min}$ fails. After adopting the JFNK method, a disturbance value δ^* in (4) is saved if it results in a worse cascading failure (*i.e.*, $J(\delta^*, x_m, y_m) < J(\delta, x_m, y_m)$). The above process does not terminate until the maximum iterative step l_{\max} is reached. For the assessment of the proposed CIA, it is important to roughly estimate the convergence accuracy of δ^* according to the following theoretical results.

Proposition 3.2. *With the CIA in Table 1, the increment $\Delta \delta$ is upper bounded by*

$$\|\Delta \delta\| \leq \varepsilon_{\min} \cdot (\|z^0\| + c \cdot s_{\max}), \tag{20}$$

where z^0 denotes the initial value for the unknown vector z in the numerical algorithm, and s_{\max} refers to the maximum iteration steps.

Table 1: Contingency Identification Algorithm.

Initialize: l_{\max} , ϵ_{\min} , ϵ_0 , and $l = 0$, $\delta = \mathbf{0}$

Goal: δ and $J(\delta, x_m, y_m)$

- 1: **while** ($l < l_{\max}$)
- 2: $s = 0$
- 3: **while** ($\epsilon_s > \epsilon_{\min}$)
- 4: Calculate the residual $\mathbf{r}^s = -\mathcal{S}(\mathbf{z}^s) - \tilde{\mathcal{J}}(\mathbf{z}^s) \cdot \Delta \mathbf{z}_0^s$
- 5: Construct the Krylov subspace K_i in (14)
- 6: Approximate $\tilde{\mathcal{J}}(\mathbf{z}^s)^j \mathbf{r}^s$ in (15) using (16)
- 7: Compute λ_j in (15) with the GMRES method
- 8: Compute $\Delta \mathbf{z}^s$ with (15)
- 9: $\mathbf{z}^{s+1} = \mathbf{z}^s + \Delta \mathbf{z}^s$
- 10: $\epsilon_{s+1} = \|\Delta \mathbf{z}^s\| / \|\mathbf{z}^s\|$
- 11: $s = s + 1$
- 12: **end while**
- 13: Update δ_l^* and $J(\delta_l^*, x_m, y_m)$
- 14: **if** ($J(\delta_l^*, x_m, y_m) < J(\delta, x_m, y_m)$)
- 15: $\delta = \delta_l^*$
- 16: **end if**
- 17: $l = l + 1$
- 18: **end while**

Proof. According to the CIA, we have the following inequality

$$\frac{\|\Delta \mathbf{z}^s\|}{\|\mathbf{z}^s\|} \leq \epsilon_{\min} \quad (21)$$

after adopting the JFNK method. In addition, it follows from the updating law $\mathbf{z}^{s+1} = \mathbf{z}^s + \Delta \mathbf{z}^s$ that $\mathbf{z}^s = \mathbf{z}^0 + \sum_{i=0}^{s-1} \Delta \mathbf{z}^i$, which allows us to obtain

$$\begin{aligned} \|\Delta \mathbf{z}^s\| &\leq \epsilon_{\min} \cdot \|\mathbf{z}^s\| \\ &= \epsilon_{\min} \cdot \left\| \mathbf{z}^0 + \sum_{i=0}^{s-1} \Delta \mathbf{z}^i \right\| \\ &\leq \epsilon_{\min} \cdot \left(\|\mathbf{z}^0\| + \sum_{i=0}^{s-1} \|\Delta \mathbf{z}^i\| \right) \\ &\leq \epsilon_{\min} \cdot (\|\mathbf{z}^0\| + c \cdot s_{\max}), \end{aligned} \quad (22)$$

due to $\|\Delta \mathbf{z}^s\| \leq c$ and $s \leq s_{\max}$. Moreover, it follows from $\|\Delta \delta\| \leq \|\Delta \mathbf{z}^s\|$ that we have

$$\|\Delta \delta\| \leq \epsilon_{\min} \cdot (\|\mathbf{z}^0\| + c \cdot s_{\max}), \quad (23)$$

which completes the proof. \square

Remark 3.2. According to the CIA in Table 1, the value of cost function $J(\delta^*, x_m, y_m)$ decreases monotonically as the iteration step l_{\max} increases. Considering that $J(\delta^*, x_m, y_m)$ is normally designed to have a lower bound (i.e., $J(\delta^*, x_m, y_m) \geq 0$), $J(\delta^*, x_m, y_m)$ converges to a local minimum, and this enables us to obtain the most disruptive contingency δ^* .

Remark 3.3. The time efficiency of Krylov subspace method is mainly related to the dimension of the system (4) instead of the size of power systems. Note that the dimension of the system (4) is constant and it does not depend on the size of power systems. Thus, Krylov subspace method is applicable to the problem of identifying the contingencies in large-scale power systems.

4 Case Study for Validating the Proposed Approach

In this section, both the DC power flow model and the AC power flow model with transient process are adopted to validate the proposed identification approach. First of all, a DC power flow model is introduced to characterize the branch outage sequence of power grids with flexible alternating current transmission system (FACTS) devices, high-voltage direct current (HVDC) links and protective relays. The mathematical descriptions of these components are presented in the Appendix. Then the CIA in

Table 1 is implemented to search for the disruptive contingencies on selected branches of IEEE 118 Bus System [29]. Moreover, the statistical analysis is conducted to investigate the effect of random factors on the identification of disruptive contingencies. The DC power flow model allows us to investigate the effect of time delay of protective relays on cascading failures.

Besides the DC power flow model, dynamical simulations are also performed using the Cascading Outage Simulator with Multiprocess Integration Capabilities (COSMIC) model. The COSMIC model takes into account the AC power flow, transient process, multiple types of load models, the generator dynamics described by differential equations, and practical protective relays for stress mitigation [11]. Disruptive contingencies are identified by the CIA on the IEEE 39 Bus System. Matlab codes for numerical simulation on both cascade models are available [30, 31].

4.1 Cascade model based on the DC power flow

The DC power flow model is adopted to describe the cascading failure process of power transmission system. When power systems are subject to the disruptive contingencies, the FACTS devices adjust the branch admittance to balance the power flow for relieving the stresses. If the stresses are not eliminated, protective relays will be activated to sever the overloading branches on the condition that the timer of circuit breakers runs out of the preset time [11]. The outage of overloading branches may result in the severer stress of power systems and lead to further branch outages. The DC power flow equation is employed in order to ensure the computational efficiency and avoid the numerical non-convergence [11]. The evolution time of cascading failure is introduced to allow for the time factor of cascading blackouts. Note that the time interval between two consecutive cascading steps basically depends on the preset time of the timer in protective relays [11]. Thus, the evolution time of cascading failure is roughly estimated by $t = kT$ at the k -th cascading step, and T denotes the preset time of the timer in protective relays. The steady-state power flow on branches updates with the change of power network topology. During the cascades, the time delay of protective relays allows the FACTS devices to adjust the branch impedance, which can be described by differential equations. The integration of the DC power flow model with differential equations serves to characterize power system cascades.

4.2 Parameter setting for the DC power flow model and CIA

Per-unit system is adopted with the base value of 100 MVA in numerical simulations, and the power flow threshold for each branch is 5% larger than the normal power flow on each branch without any contingencies. The power flow on each branch is close to the saturation, although it does not exceed

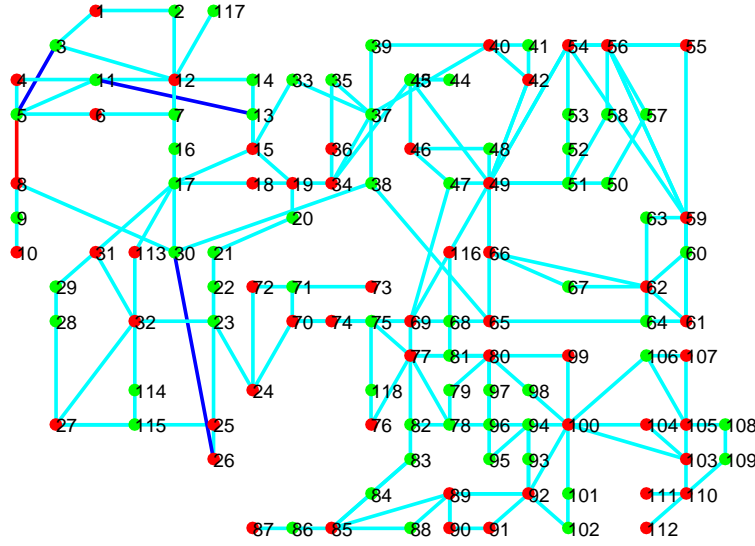


Figure 2: Initial state of IEEE 118 Bus System. Red balls denote the generator buses, while green ones stand for the load buses. Cyan lines represent the branches of power systems. In addition, the red line is selected as the disturbed branch, and three blue lines are the HVDC links, including Branch 4, Branch 16 and Branch 38.

their respective thresholds. Thus, the power system is sensitive to disruptive contingencies. The cost function in the optimization problem (3) is defined as $\|P_e(\delta, P^m, Y_p^m)\|^2$ to minimize the total power flow on branches, where P_e represents the vector of power flow on branches. P^m and Y_p^m denote the vector of injected power on buses and vector of branch admittance at the end of cascading failure, respectively. The injected power on generator buses and load buses are constant in the DC power flow model. The maximum iterative step l_{\max} is equal to 10 in the CIA. Other parameters are given as follows: $\varepsilon = 10^{-2}$ in Equation (16), $\varepsilon_{\min} = 10^{-8}$ in the JFNK method. Branch 8 (i.e., the red link connecting Bus 5 to Bus 8 in Figure 2) is randomly selected as the disturbed element of power networks. The lower and upper bounds of initial disturbances on Branch 8 are given by $\underline{\delta} = 0$ and $\bar{\delta} = 37.45$, respectively. Note that the upper bound of initial disturbances directly causes the branch outage. And the total number of cascading steps is $m = 12$. For simplicity, the same values are specified for the parameters of three HVDC links as follows: $R_{ci} = R_{cr} = R_L = 0.1$, $\alpha = \pi/15$ and $\gamma = \pi/4$. Regarding the FACTS devices, we set $X_{\min,i} = 0$, $X_{\max,i} = 10$ and $X_i^* = 0$ for the TCSC, and $K_P = 4$, $K_I = 3$ and $K_D = 2$ for the PID controller via the trial-and-error method. In addition, the reference power flow $P_{e,i}^*$ accounts for 80% with respect to the power flow capacity of relevant branches.

4.3 Numerical simulation and validation

Numerical simulations are conducted on the IEEE 118 Bus System by using the CIA and the DC power flow model with different time delays of protective relays. Figure 2 shows the initial state of IEEE 118 Bus System in the normal condition, and it includes 53 generator buses, 64 load buses, 1 reference bus (i.e., Bus 69) and 186 branches. And the HVDC links are denoted by blue lines, which include Branch 4 connecting Bus 3 to Bus 5, Branch 16 connecting Bus 11 to Bus 13 and Branch 38 connecting Bus 26 to Bus 30. In practice, the time delay of circuit breaker ranges from 0.3s to 1s with the consideration of reclosing time of circuit breakers [32]. In the simulations, two preset values of the timer are taken into consideration for protective relays ($T = 0.5s$ and $T = 1s$). The CIA is carried out to search for the initial contingency that results in the catastrophic cascading failures of power systems (i.e., relatively small values of cost function $\|P_e(\delta, P^m, Y_p^m)\|^2$). For the case without the FACTS devices, the computed magnitude of disturbance on Branch 8 is 37.45, which exactly leads to the outage of Branch 8. To be exact, the disturbance magnitude refers to the magnitude of the change of branch susceptance caused by the contingency. For the case with the FACTS devices and the preset time of the timer $T = 0.5s$, the disturbance magnitude identified by the CIA is 36.77, while it is 35.98 for $T = 1s$. Thus, the CIA is able to identify the continuous change of branch impedance in power systems, in addition to the direct branch outage. The above results demonstrate the advantage of the proposed method over existing methods that can only identify the direct branch outage as the disruptive contingency. In the simulations, it takes around 5s to implement the JFNK method for identifying the initial contingencies of IEEE 118 Bus System.

Next, we validate the proposed identification approach by adding the computed magnitude of disturbances on Branch 8 of IEEE 118 Bus Systems. Specifically, Figure 3 demonstrates the final state of IEEE 118 Bus System with no FACTS devices and with the preset time of circuit breaker $T = 1s$. The cascading process terminates with 95 outage branches and the value of cost function is 53.28 after 16 seconds, and the system collapses with 42 islands in the end. These 42 islands include 24 isolated buses and 18 subnetworks. In contrast, Figure 4 presents the final configuration of IEEE 118 Bus Systems with the protection of the FACTS devices and with the preset time $T = 0.5s$. The cascading process ends up with 40 outage branches and the value of cost function is 102.56 after 10 seconds, and the power system is separated into 17 islands, which include 6 subnetworks and 11 isolated buses. Figure 5 presents the final state of power systems with FACTS devices and $T = 1s$. It is observed that the power network is eventually split into 3 islands (Bus 14, Bus 16 and a subnetwork composed of all other buses) with only 6 outage branches and the cost function of 153.69. Note that the initial contingencies identified by the CIA

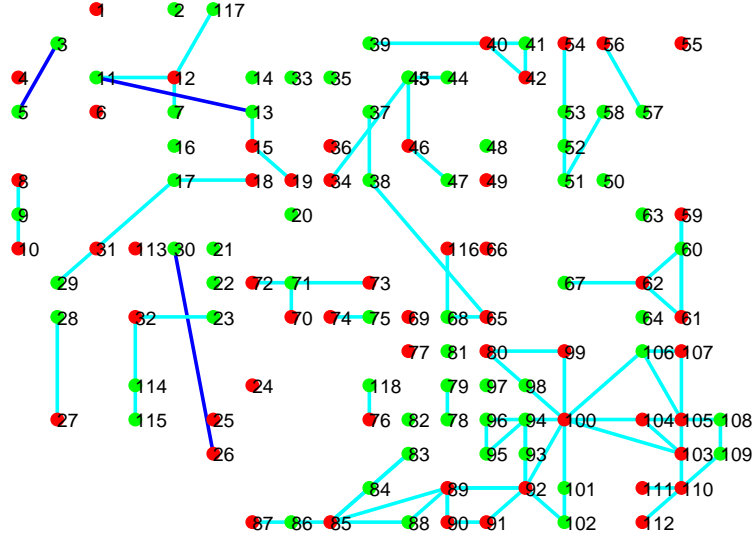


Figure 3: Final configuration of IEEE 118 Bus System without FACTS devices.

fail to cause the outage of Branch 8 in the end for both $T = 0.5s$ and $T = 1s$. The above simulation results demonstrate the advantage of the FACTS devices in preventing the propagation of cascading outages. A larger preset time of timer enables the FACTS devices to sufficiently adjust the branch admittance in response to the overload stress. As a result, the less severe damages are caused by the contingency with the larger preset time of timer.

Figure 6 presents the time evolution of branch outages in the IEEE 118 Bus System after adding disruptive contingencies on Branch 8 in three different scenarios. The cyan squares denote the number of outage branches with no FACTS devices and $T = 1s$, while the green and blue ones refer to the numbers of outage branches with the FACTS devices and with $T = 0.5s$ and $T = 1s$, respectively. The contingencies identified by the CIA are added to change the admittance of Branch 8 at $t = 0s$. With no FACTS devices, the cascading outage of branches propagates quickly from $t = 2s$ to $t = 10s$ and terminates at $t = 16s$. When the FACTS devices are adopted and the preset time of timer is $T = 0.5s$, the cascading failure starts at $t = 2s$ and speeds up till $t = 8s$ and stops at $t = 10s$. For $T = 1s$, the cascading outage propagates slowly due to the larger preset time of timer and comes to an end with only 6 outage branches at $t = 8s$. Together with protective relays and HVDC links, the FACTS devices succeed in protecting power systems against blackouts by adjusting the branch impedance in real time. More precisely, the number of outage branches decreases by 57.9% with FACTS devices and $T = 0.5s$ and decreases by 93.7% with FACTS devices and $T = 1s$.

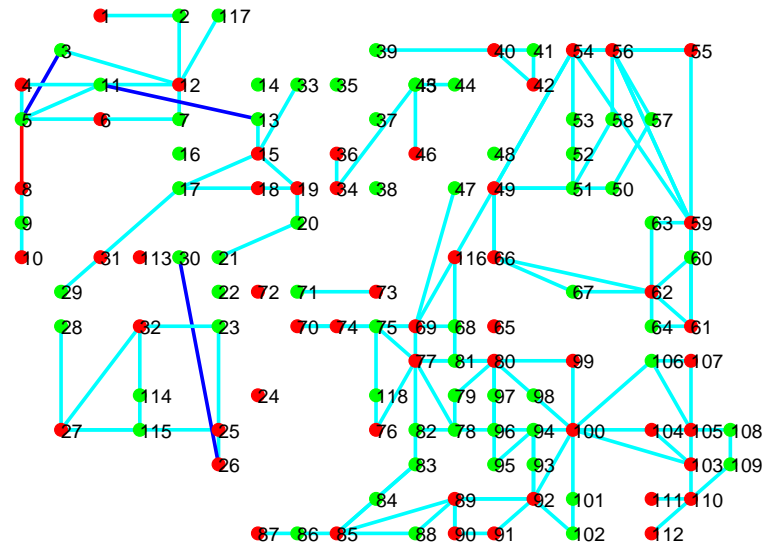


Figure 4: Final configuration of IEEE 118 Bus System with FACTS devices and $T = 0.5s$.

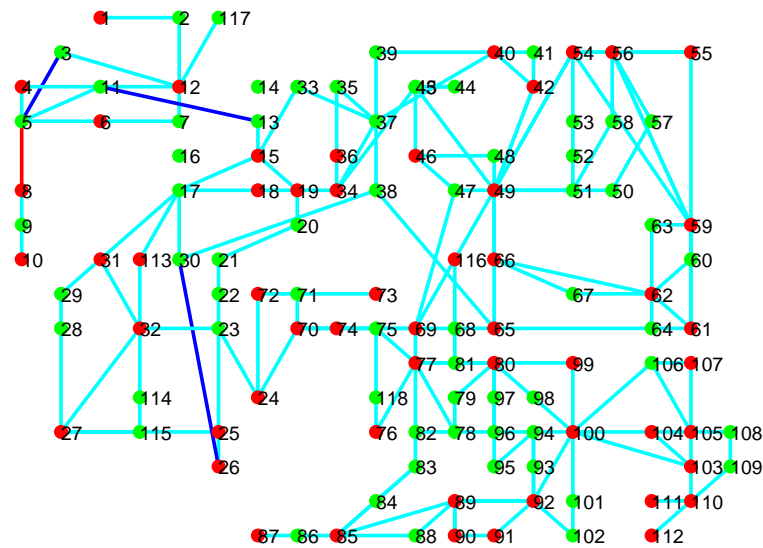


Figure 5: Final configuration of IEEE 118 Bus System with FACTS devices and $T = 1s$.

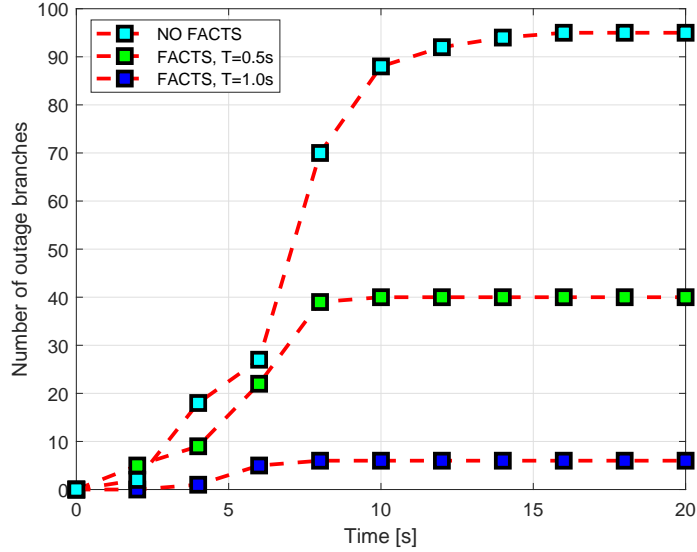


Figure 6: Time evolution of outage branches during cascades.

4.4 Statistical analysis

To further validate the proposed approach for the DC power flow model, statistical analysis is conducted by taking into account random factors (*e.g.*, hidden failures of branches). If one branch is exposed to line tripping through a common bus, it is more likely to be tripped incorrectly due to hidden failures [33]. Suppose the probability of an exposed line tripping incorrectly is 0.05, and the time delay of protective relay is 0.5s. Then multiple cascading failure paths could be generated by adding the initial contingency on the selected branch. The initial contingency causes the change of branch admittance or the direct branch outage. In the simulations, 5 branches (*i.e.*, Branch 5, Branch 26, Branch 45, Branch 64, and Branch 108) are randomly selected on IEEE 118 Bus System, and the CIA is implemented for 100 times on each selected branch to identify the initial contingency. Table 2 presents the statistics on the cascading failures identified by the CIA in terms of initial contingencies and the values of cost function. In this table, J^* denotes the minimum value of cost function in the 100 simulation trials, and δ^* refers to the initial contingency that leads to the minimum value of cost function J^* . In addition, μ_δ and σ_δ represent the mean value and standard deviation of the initial contingencies δ identified by the CIA, respectively. Similarly, μ_J and σ_J denote the mean value and standard deviation of values of cost function at the end of cascades by adding the identified initial contingencies, respectively. Note that the identified initial contingency $\delta^* = 25.38$ on Branch 26 results in the direct branch outage (*i.e.*, sever Branch 26). In contrast, the identified contingencies δ^* on other four branches (Branches 5, 45, 64 and 108) actually

give rise to the change of their respective branch admittances instead of the direct branch outages, which subsequently causes the overload and outage of other branches in power systems. It is observed that the disturbance $\delta^* = 3.66$ on Branch 64 results in the worst-case cascading failures of the five identified contingencies δ^* in terms of the values of cost function J^* . In addition, the identified contingencies on Branch 64 have a relatively small standard deviation $\sigma_\delta = 1.61$, which implies that Branch 64 is sensitive to catastrophic cascading failures within a relative small range of initial contingencies. On the whole, the identified contingencies on Branch 108 can lead to the worst-case cascading failures in terms of mean values μ_J with the smallest standard deviation $\sigma_J = 93.21$.

Table 2: Statistics on Cascading Failures Identified by the CIA

Branch ID	Bus ID	δ^*	J^*	μ_δ	σ_δ	μ_J	σ_J
5	5-6	14.93	91.68	8.95	6.46	190.83	94.25
26	15-19	25.38	69.51	13.36	9.35	206.52	100.22
45	19-34	3.41	89.84	2.09	1.64	237.52	107.21
64	46-48	3.66	63.82	3.32	1.61	192.38	96.35
108	69-70	3.67	86.35	4.18	2.43	176.75	93.21

4.5 Applications to other cascade models

The proposed identification approach is also applied to more complicated cascade models. To demonstrate its efficacy, the CIA is implemented to identify the initial contingencies on the IEEE 39 Bus System, and the COSMIC model is adopted to describe the cascading failure process [11]. In the simulation, Branch 2 is randomly selected to identify the initial disruptive contingencies, and the parameter setting remains unchanged [11]. In addition, the cost function J is the same as that in the DC power flow model and it is computed based on the real power flow. The cascades last for 10 seconds and Branch 35 is tripped by accident at the 3rd second. The tripping of Branch 35 may result from the error of human operator or hidden failure of power system devices. The CIA allows to obtain the initial disruptive contingency $\delta^* = 3.3$ with the cost function $J = 575.72$ after 10 iterations. It is demonstrated that the identified initial contingency on Branch 2 initially results in the tripping of Branch 3 at $t = 0.001s$ and subsequently a sequence of under voltage load shedding (UVLS) at Buses 3, 4, 7, 8, 12, 15, 16, 18, and 27. Then Branch 2 is tripped at $t = 0.86s$, which leads to the UVLS at Bus 26 and Bus 31 in succession. Afterwards, Branch 35 is tripped at $t = 3s$, which causes the failure of numeric solver in the

COSMIC model and the termination of simulations. Compared with existing identification approaches, the proposed approach is able to identify the disruptive contingencies that give rise to the continuous change of branch admittance, in addition to the direct branch outages. Moreover, it is applied to both the simplified DC power flow models as well as the complicated cascade models that involve the AC power flow, transient process, generator dynamics, and protective relays.

5 Conclusions

This paper investigated the problem of identifying the disruptive contingencies that cause catastrophic cascading blackout. A general optimization formulation was proposed to describe the cascading failure. In addition, a numerical algorithm based on JFNK method was presented to solve the optimization problem. Numerical simulations were carried out to validate the proposed identification approach for different cascade models. The proposed identification algorithm allows to detect some nontrivial contingencies that result in the catastrophic cascading failure, in addition to the direct branch outage. Future work may include the effect of model uncertainty on the identification of disruptive contingencies.

Acknowledgment

The authors wish to thank Shuhan Yao at School of Electrical and Electronic Engineering, Nanyang Technological University, Singapore for all the insightful discussions and constructive suggestions. This work is partially supported by the Future Resilient Systems Project at the Singapore-ETH Centre (SEC), which is funded by the National Research Foundation of Singapore (NRF) under its Campus for Research Excellence and Technological Enterprise (CREATE) program. It is also supported by Ministry of Education of Singapore under Contract MOE2016-T2-1-119.

Appendix

In practice, electrical power devices such as FACTS, HVDC links and protective relays serve as the major protective barrier against cascading blackouts [34, 35, 36]. This section presents the component models of power grids, which include FACTS in Appendix A, HVDC links in Appendix B and Protective relays in Appendix C.

Appendix A: FACTS devices

FACTS devices can greatly enhance the stability and transmission capability of power systems. As an effective FACTS device, TCSC has been widely installed to control the branch impedance and relieve system stresses. The dynamics of TCSC is described by a first order dynamical model [37]

$$T_{C,i} \frac{dX_{C,i}}{dt} = -X_{C,i} + X_i^* + u_i, \quad X_{\min,i} \leq X_{C,i} \leq X_{\max,i} \quad (24)$$

where X_i^* refers to its reference reactance of Branch i for the steady power flow. $X_{\min,i}$ and $X_{\max,i}$ are the lower and upper bounds of the branch reactance $X_{C,i}$ respectively and u_i represents the supplementary control input, which is designed to stabilize the disturbed power system [38]. For simplicity, PID controller is adopted to regulate the power flow on each branch

$$u_i(t) = K_P \cdot e_i(t) + K_I \cdot \int_0^t e_i(\tau) d\tau + K_D \cdot \frac{de_i(t)}{dt} \quad (25)$$

where K_P , K_I and K_D are tunable coefficients, and the error $e_i(t)$ is given by

$$e_i(t) = \begin{cases} P_{e,i}^* - |P_{e,i}(t)|, & |P_{e,i}(t)| \geq P_{e,i}^*; \\ 0, & \text{otherwise.} \end{cases} \quad (26)$$

Here, $P_{e,i}^*$ and $P_{e,i}(t)$ denote the reference power flow and the actual power flow on Branch i , respectively. Note that TCSC fails to function when the transmission line is severed.

Appendix B: HVDC links

HVDC links work as a protective barrier to prevent the propagation of cascading outages in practice, and it is normally composed of a transformer, a rectifier, a DC line and an inverter. Actually, the rectifier terminal can be regarded as a bus with real power consumption P_r , while the inverter terminal can be treated as a bus with real power generation P_i . The direct current from the rectifier to the inverter is computed as follows [39]

$$I_d = \frac{3\sqrt{3}(\cos \alpha - \cos \gamma)}{\pi(R_{cr} + R_L - R_{ci})}, \quad (27)$$

where $\alpha \in [\pi/30, \pi/2]$ denotes the ignition delay angle of the rectifier, and $\gamma \in [\pi/12, \pi/9]$ represents the extinction advance angle of the inverter. R_{cr} and R_{ci} refer to the equivalent communicating resistances for the rectifier and inverter, respectively. Additionally, R_L denotes the resistance of the DC transmission line. Thus the power consumption at the rectifier terminal is

$$P_r = \frac{3\sqrt{3}}{\pi} I_d \cos \alpha - R_{cr} I_d^2, \quad (28)$$

and at the inverter terminal is

$$P_i = \frac{3\sqrt{3}}{\pi} I_d \cos \gamma - R_{ci} I_d^2 = P_r - R_L I_d^2. \quad (29)$$

Note that P_r and P_i keep unchanged when α and γ are fixed.

Appendix C: Protective relay

The protective relays are indispensable components in power systems protection and control. When the power flow exceeds the given threshold of the branch, the timer of circuit breaker starts to count down from the preset time [11]. Once the timer runs out of the preset time, the transmission line is severed by circuit breakers and its branch admittance becomes zero. Specifically, a step function is designed to reflect the physical characteristics of branch outage as follows

$$g(P_{e,i}, b_i) = \begin{cases} 0, & |P_{e,i}| > b_i \text{ and } t_c > T; \\ 1, & \text{otherwise.} \end{cases} \quad (30)$$

where T is the preset time of the timer in protective relays, and t_c denotes the counting time of the timer. In addition, $P_{e,i}$ denotes the power flow on Branch i with the threshold b_i .

References

- [1] S. Masood, Rebels tied to blackout across most of pakistan, *New York Times*, January 25, 2015.
- [2] Y. Shao, Y. Tang, J. Yi, and A. Wang, Analysis and lessons of blackout in Turkey power grid on March 31, 2015, *Automation of Electric Power Systems*, vol. 40, pp. 9-14, 2016.
- [3] M. Nagpal, T. Martinich, Z. Jiao, S. Manuel, H. Zhang, and A. Alimardani, Lessons learned from a regional system blackout and restoration in BC Hydro. *IEEE Transactions on Power Delivery*, vol. 33, no. 4, pp. 1954-1961, 2018.
- [4] B. Zhou, Q. Chen, and D. Yang, On the power system large-scale blackout in Brazil, *Power Generation Technology*, vol. 39, no. 2 pp. 97-105, 2018.
- [5] H. Sun, T. Xu, Q. Guo, Y. Lo, W. Lin, J. Y, and W. Li, Analysis on blackout in Great Britain power grid on August 9th, 2019 and its enlightenment to power grid in China. *Proceeding of the CSEE*, vol. 39, no. 21, pp. 6183-6191, 2019.

- [6] J. McLinn, Major power outages in the US, and around the world, *Annual Technology Report of IEEE Reliability Society*, 2009.
- [7] US-Canada Power System Outage Task Force, Final Report on the August 14, 2003 Blackout in the United States and Canada: Causes and Recommendations, 2004.
- [8] Final Report of the Investigation Committee on the 28 September 2003 Blackout in Italy, UCTE, 2004.
- [9] S. Larsson and E. Ek, The blackout in Southern Sweden and Eastern Denmark, September 23, 2003, Proceedings of IEEE PES General Meeting, Denver, CO, 2004.
- [10] C. Zhai, H. Zhang, G. Xiao, and T. Pan, A model predictive approach to preventing cascading failures of power systems, *International Journal of Electrical Power & Energy Systems*, vol. 113, pp. 310-321, 2019.
- [11] J. Song, et al, Dynamic modeling of cascading failure in power systems, *IEEE Transactions on Power Systems*, vol. 31, no. 3, pp. 2085-2095, 2016.
- [12] J. Yan, Y. Tang, H. He, and Y. Sun, Cascading failure analysis with DC power flow model and transient stability analysis, *IEEE Transactions on Power Systems*, vol. 30, no. 1, pp. 285-297, 2015.
- [13] Q. Chen, and J. McCalley, Identifying high risk n-k contingencies for online security assessment, *IEEE Transactions on Power Systems*, vol. 20, no. 2, pp. 823-834, 2005.
- [14] C. Davis, and T. Overbye, Multiple element contingency screening, *IEEE Transactions on Power Systems*, vol. 26, no. 3, pp. 1294-1301, 2011.
- [15] V. Donde, V. Lopez, B. Lesieutre, A. Pinar, C. Yang, and J.Meza, Severe multiple contingency screening in electric power systems, *IEEE Transactions on Power Systems*, vol. 23, no. 2, pp. 406-417, 2008.
- [16] D. Bienstock and A. Verma, The n-k problem in power grids: New models, formulations, and numerical experiments, *SIAM Journal on Optimization*, vol. 20, no. 5, pp. 2352-2380, 2010.
- [17] C. Rocco, J. Ramirez-Marquez, D. Salazar, and C. Yajure, Assessing the vulnerability of a power system through a multiple objective contingency screening approach, *IEEE Transactions on Reliability*, vol. 60, no. 2, pp. 394-403, 2011.

- [18] M. Eppstein, and P. Hines, A “random chemistry” algorithm for identifying collections of multiple contingencies that initiate cascading failure, *IEEE Transactions on Power Systems*, vol. 27, no. 3, pp. 1698-1705, 2012.
- [19] C. Zhai, H. Zhang, G. Xiao, and T. Pan, An optimal control approach to identify the worst-case cascading failures in power systems, *IEEE Transactions on Control of Network Systems*, DOI: 10.1109/TCNS.2019.2930871, July 2019.
- [20] H. Beaty, *Handbook of Electric Power Calculations*, McGraw-Hill, 2001.
- [21] P. Hines, and P. Rezaei, Cascading failures in power systems, *Smart Grid Handbook*, pp. 1-20, 2016.
- [22] O. Mangasarian, *Nonlinear programming*, SIAM, 1994.
- [23] K. Taedong, S. Wright, D. Bienstock, and S. Harnett, Analyzing vulnerability of power systems with continuous optimization formulations, *IEEE Transactions on Network Science and Engineering*, vol. 3, no. 3, pp. 132-146, 2016.
- [24] D. Knoll, and D. Keyes, Jacobian-free Newton-Krylov methods: a survey of approaches and applications, *Journal of Computational Physics*, vol. 193, no. 2, pp. 357-397, 2004.
- [25] Y. Saad, and H. Martin, GMRES: A generalized minimal residual algorithm for solving nonsymmetric linear systems, *SIAM Journal on Scientific and Statistical Computing*, vol. 7, no. 3, pp. 856-869, 1986.
- [26] P. Brown, and Y. Saad, Hybrid Krylov methods for nonlinear systems of equations, *SIAM Journal on Scientific and Statistical Computing*, vol. 11, no. 3, pp. 450-481, 1990.
- [27] J. Ortega, and W. Rheinboldt, *Iterative Solution of Nonlinear Equations in Several Variables*, SIAM, Philadelphia, 2000
- [28] T. Chan, and K. Jackson, Nonlinearly preconditioned Krylov subspace methods for discrete Newton algorithms, *SIAM Journal on Scientific and Statistical Computing*, vol. 5, no. 3, pp. 533-542, 1984.
- [29] R. Zimmerman, C. Murillo-Sánchez, and R. Thomas, Matpower: Steady-state operations, planning and analysis tools for power systems research and education, *IEEE Transactions on Power Systems*, vol. 26, no. 1, pp. 12-19, 2011.

- [30] <https://github.com/Chaocas/cascading-faiulure>.
- [31] <https://github.com/ecotillasanchez/cosmic>.
- [32] PJM Relay Subcommittee, Protective Relaying Philosophy and Design Guidelines, July 12, 2018.
- [33] J. Thorp, A. Phadke, S. Horowitz, and C. Tamronglak, Anatomy of power system disturbances: importance sampling, *International Journal of Electrical Power & Energy Systems*, vol. 20, no. 2, pp.147-152, 1998.
- [34] S. Tamronglak, S. Horowitz, A. Phadke, and J. Thorp, Anatomy of power system blackouts: preventive relaying strategies, *IEEE Transactions on Power Delivery*, vol. 11, no. 2, pp. 708-715, 1996.
- [35] L. Kirschner, D. Retzmann, and G. Thumm, Benefits of FACTS for power system enhancement, IEEE/PES Transmission and Distribution Conference and Exposition: Asia and Pacific, 2005.
- [36] O. Mousavi, L. Bizumic, and R. Cherkaoui, Assessment of HVDC grid segmentation for reducing the risk of cascading outages and blackouts, 2013 IREP Symposium Bulk Power System Dynamics and Control-IX Optimization, Security and Control of the Emerging Power Grid, Rethymno, Greece, 25-30 Aug. 2013.
- [37] J. Paserba, et al, A thyristor controlled series compensation model for power system stability analysis, *IEEE Transactions on Power Delivery*, vol. 10, no. 3, pp. 1471-1478, 1995.
- [38] K. Son, and J. Park, On the robust LQG control of TCSC for damping power system oscillations, *IEEE Transactions on Power Systems*, vol. 15, no. 4, pp. 1306-1312, 2000.
- [39] P. Kundur, N. Balu, and M. Lauby. *Power System Stability and Control*, vol. 7, New York: McGraw-hill, 1994.